

**Moshe Brand**  
**Michael Ryvkin**<sup>1</sup>  
e-mail: arikr@eng.tau.ac.il

Department of Solid Mechanics, Materials and  
Systems, Faculty of Engineering, Tel Aviv  
University, Ramat Aviv 69978, Israel

**Shmuel Einav**  
Department of Biomedical Engineering, Faculty of  
Engineering, Tel Aviv University, Ramat Aviv  
69978, Israel

**Leonid Slepyan**  
Department of Solid Mechanics, Materials and  
Systems, Faculty of Engineering, Tel Aviv  
University, Ramat Aviv 69978, Israel

# The Cardiocoil Stent-Artery Interaction

*An analytical approach for the mechanical interaction of the self-expanding Cardiocoil stent with the stenosed artery is presented. The damage factor as the contact stress at the stent-artery interface is determined. The stent is considered as an elastic helical rod having a nonlinear pressure-displacement dependence, while the artery is modeled by an elastic cylindrical shell. An influence of a moderate relative thickness of the shell is estimated. The equations for both the stent and the artery are presented in the stent-associated helical coordinates. The computational efficiency of the model enabled to carry out a parametric study of the damage factor. Comparative examinations are conducted for the stents made of the helical rods with circular and rectangular cross sections. It was found, in particular, that, under same other conditions, the damage factor for the stent with a circular cross section may be two times larger than that for a rectangular one. [DOI: 10.1115/1.1871194]*

**Keywords:** Self-Expanding Stent, Damage Factor, Analytic Solution, Parametric Study

## 1 Introduction

The unacceptably high restenosis rate [1] after the stenting procedure stimulated many studies of the topic in order to understand the mechanics involved in the process. At the final stage of the procedure, the stent interacts with the artery by applying some pressure at the contact area. This pressure has a considerable influence on the stress state within the artery walls [2]. When the stent is unsuitable and the pressure is too high it may cause local injury of the artery as well as high stresses in the arterial wall. Both these factors increase the risk for a restenosis, including a narrowing of the lumen. A correlation between the suboptimal stent dilatation with the occurrence of restenosis was reported by Akiyama [3]. Injury of the artery was also shown to cause inflammation resulting in rapid multiplication of cells and the formation of a layer (neointima), producing a narrowing of the lumen [4]. Rachev [5] and Rachev et al. [6] investigated the stress dependent remodeling of the vessel wall as possible causes of restenosis.

The stress state in the artery that had been injured after stenting depends upon its geometry and the mechanical properties in combination with the properties of the stent. The stiffness and other mechanical properties of stents were investigated by many researchers. Most of the studies are based either on the experimental approach [7–10] or on the numerical modeling [11,12]. Analytical models were also used in a number of studies to verify the experiments [13,14].

Stent-artery interaction which requires a model that is capable of simultaneously evaluating the stent and the artery, however, has been less investigated. Holzapfel et al. [15] used a numerical model for the balloon-expanded Palmaz-Schatz stent: the authors considered the problem in a framework of finite strains and the arterial wall being composed of several layers with different properties. Auricchio et al. [16] also investigated the interaction of a balloon expanded stent with an artery and suggested a modified design in order to reduce the nonuniformity of the contact stress distribution.

The goal of the present research is to investigate theoretically the main features of the mechanical interaction of an artery with a self-expanding stent undergoing only elastic deformations during

deployment. We concentrate on Cardiocoil nitinol stent [17]. The experimental and clinical performance of this stent was extensively studied by several authors [17–21]. The crucial role of appropriate stent sizing was emphasized by Hong et al. [20]. The Cardiocoil stent has a relatively simple geometric structure suitable for the purposes of mathematical description. This enabled us to develop an efficient analytical interaction model convenient for the analysis. Specifically, our model demonstrates the influence of the geometric and elastic parameters of the problem on the *damage factor* defined by the stresses appearing at the interface contact zone. Knowledge of this factor and, in particular, its dependence upon the stent-artery radial mismatch is important for choosing the correct size and type of Cardiocoil stent for each patient. In addition, the obtained analytic solution could provide convenient benchmark problems to be used as guidelines in the search for more accurate and, consequently, more advanced numerical approaches.

The analytical model of an elastic circular cylinder representing the artery is given in the next section. Section 3 describes a stent which is considered to represent an elastic curvilinear rod. The nonlinear stent-artery interaction problem is formulated and solved in Sec. 4. The numerical results are presented in Sec. 5, followed by the concluding remarks.

## 2 Artery Model

The assumption that an arterial wall can be modeled as a homogeneous elastic layer and an artery as a cylindrical membrane or a hollow elastic cylinder was accepted by many authors. Holzapfel et al. [22] considered this model in the framework of a large strain analysis. Rachev [5] used a different two-layered model, while Auricchio et al. [16] considered the artery and the plaque as dissimilar homogeneous isotropic materials. In order to reveal the main features of the stent-artery interaction in the present study we employed a relatively simple model in which the artery is considered as being a circular hollow cylinder made of homogeneous elastic material. As such, the geometry of the cylinder is completely defined by the wall thickness  $h$  and the radius of the middle surface  $R$  (Fig. 1). The elastic properties of the artery walls are described by the Young modulus  $E$  and the Poisson ratio  $\nu$ .

Note that the analytical approach used here is still valid for a more sophisticated artery model, for example, for a three-layer

<sup>1</sup>To whom correspondence should be addressed.

Contributed by the Bioengineering Division for publication in the JOURNAL OF BIOMECHANICAL ENGINEERING. Manuscript received: January 27, 2004. Final manuscript received: September 10, 2004. Associate Editor: Fumihiko Kajiya.

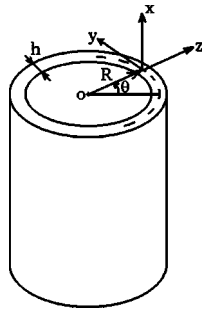


Fig. 1 Artery segment and cylindrical coordinate system

model corresponding to Intima, Media, and Advestitia or for a multilayer model, while the simplest formulation adopted in the present paper gives us the first approximation.

The solution of the stent-artery interaction problem hinges on the knowledge of the compliance of both constituents of the system. The radial compliance of the cylinder subjected to the inner pressure along the helical strip is calculated in two steps. First, the problem on the corresponding thin-walled shell with helical loading is solved analytically. Then, in order to take into account the finite relative thickness of the shell, this solution is corrected by the use of numerical results of an auxiliary problem which will be specified later.

The system of curvilinear cylindrical coordinates  $x, y, z$  with  $y = R\theta$  is defined as shown in Fig. 1, and the corresponding displacements are denoted as  $u, v, w$ , respectively. The elastic behavior of the thin-walled shell subjected to normal internal pressure  $p(x, y)$  (the stent-artery contact is assumed to be frictionless) is defined by a system of three partial differential equilibrium equations with respect to  $u(x, y), v(x, y)$  and  $w(x, y)$  (see, for example, Ref. [23]).

The pressure is applied to the artery by the stent which is considered as a helical rod. Consequently, the contact zone is a helical strip of width  $b$  defined by the rod's cross section. Its location is completely determined by the angle  $\alpha$  between the  $x$  axis and the vector tangential to the helix (see Fig. 2(a)). Note, that the value  $\alpha$  corresponds to the deformed state of the stent, it will be determined during the solution of stent-artery interaction problem. Clearly

$$\alpha = \arctan \frac{2\pi R}{H} \quad (1)$$

where  $H$  is the pitch of the helix (see Fig. 2(a)).

In the present work we concentrated upon studying the deformations appearing in the middle part of the stent-artery mechanical system and did not consider the regions where the stent terminates. Consequently, the distributed loading applied to the artery is assumed to be constant along the contact strip. In this case the stress-strain state within the artery will possess the same screw symmetry as the contact helix zone itself. This fact dictates the

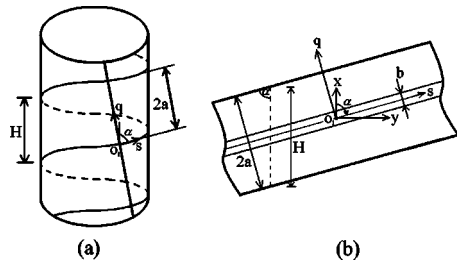


Fig. 2 Cylindrical shell with helical coordinate system (a); the shell deployed to a strip (b)

need for employing a nonstandard system of helical curvilinear coordinates for the analysis. In such a system, the radial coordinate  $z$  remains the same while the coordinates  $x, y$  are replaced by the helical coordinates  $q, s$  as two mutually orthogonal systems of helices (see Fig. 2(a)). On the cylindrical surface  $z = \text{const} = R$ , these coordinates vary within the following limits  $-a < q < a$ ,  $-\infty < s < \infty$ . The cylindrical and the helical coordinate lines on the shell surface are presented in Fig. 2(b) where the strip of the width  $2a = H \sin \alpha$  is depicted. The strip is obtained by cutting the shell along the coordinate line  $q = \text{const}$  and deploying it to a plain figure. The relations between the coordinates are given by the rotation matrix as it is seen from Fig. 2(b):

$$\begin{Bmatrix} s \\ q \end{Bmatrix} = \begin{Bmatrix} \sin \alpha & \cos \alpha \\ -\cos \alpha & \sin \alpha \end{Bmatrix} \begin{Bmatrix} y \\ x \end{Bmatrix} \quad (2)$$

For the considered symmetry the stresses and strains are periodic in  $x$  and  $y$  with the periods  $H$  and  $2\pi R$ , respectively, while they are independent of  $s$ . This allows us to consider the fields at any given  $s$  for arbitrary extended  $q$ . In such representation, the stress fields are periodic in the  $q$  direction with the period equal to  $2a$ . The radial displacements being independent of  $s$  are also periodic in  $q$ :

$$w = w(q) \quad (3)$$

Regarding the remaining two displacements  $u$  and  $v$ , one must take into account that they have components linearly depending on  $x$ , i.e.,

$$u = \tilde{u}(q) + \varepsilon_0 x \quad (4)$$

$$v = \tilde{v}(q) + \psi_0 x \quad (5)$$

where  $\varepsilon_0$  and  $\psi_0$  are the averaged strain along the  $x$  axis and the angle of torsion about this axis, respectively.

Substituting the expressions for  $x, y$  from (2) into the mentioned system of partial differential equations and using (3)–(5), after some manipulation, we obtain

$$t_1 \frac{\partial^2 \tilde{u}}{\partial q^2} - \frac{\nu^+}{2} \frac{\partial^2 \tilde{v}}{\partial q^2} \sin 2\alpha + \frac{\nu}{R} \frac{\partial w}{\partial q} \sin \alpha = 0 \quad (6)$$

$$(1 + k^2) t_2 \frac{\partial^2 \tilde{v}}{\partial q^2} - \frac{\cos \alpha}{R} \frac{\partial w}{\partial q} - \frac{\nu^+}{2} \frac{\partial^2 \tilde{u}}{\partial q^2} \sin 2\alpha + k^2 R \frac{\partial^3 w}{\partial q^3} \cos \alpha = 0 \quad (7)$$

$$\frac{\partial^4 w}{\partial q^4} + \frac{\cos \alpha}{R} \frac{\partial^3 \tilde{v}}{\partial q^3} + \frac{1}{k^2 R^3} \left[ \frac{w}{R} - \frac{\partial \tilde{v}}{\partial q} \cos \alpha + \nu \varepsilon_0 + \nu \frac{\partial \tilde{u}}{\partial q} \sin \alpha \right] = \frac{p(q)}{D_s} \quad (8)$$

$$\text{where } \nu^+ = \frac{1 + \nu}{2}, \quad k^2 = \frac{h^2}{12R^2}, \quad D_s = \frac{Eh^3}{12(1 - \nu^2)},$$

$$t_1 = \sin^2 \alpha + \nu^- \cos^2 \alpha, \quad t_2 = \nu^- \sin^2 \alpha + \cos^2 \alpha$$

It is assumed that the coordinate line  $q=0$  corresponds to the middle of the helical contact zone of width  $b$  (see Fig. 2(b)). Then, in accordance with the helical symmetry of the deformed shape of the shell, the radial displacements  $w(q)$  are represented by an even function and the nontrivial parts of the displacements tangential to the shell surface  $\tilde{u}(q)$  and  $\tilde{v}(q)$  are odd functions. Consequently, in view of the  $2a$  periodicity of these functions, it is suitable to present them by the following Fourier series:

$$\{\tilde{u}, \tilde{v}\} = \sum_{n=1}^{\infty} \{u_n, v_n\} \sin \frac{\pi n q}{a} \quad (9)$$

$$w = \sum_{n=0}^{\infty} w_n \cos \frac{\pi n q}{a} \quad (10)$$

The unknown coefficients are defined after substitution of (9) and (10) into (6)–(8) in a standard manner. Multiplication of the first two equations by the  $\sin(n\pi q/a)$  and the third one by the

$\cos(n\pi q/a)$  and integration over  $q$  yields the system of three linear algebraic equations for deriving the triple of unknown coefficients  $u_n, v_n,$  and  $w_n$  for each  $n=1, 2, \dots$ . For formulating the problem on stent artery compatibility, we are interested primarily in radial displacement. The coefficients  $w_n, n=1, 2, \dots$  are found to be

$$w_n = \frac{\nu^+ t_3 k^2 R^4 Q_n}{D_s a \{t_3(\nu^+ p_2 - \nu p_1) - 2(p_1 t_1 - \nu \nu^+ \sin^2 \alpha)[\nu t_2(1+k^2) - \nu^+ p_2 \cos^2 \alpha]\}},$$

with  $t_3 = (1+k^2)t_1 t_2 - \left(\frac{\nu^+ \sin 2\alpha}{2}\right)^2, \quad p_i = 1 + k^2 \left(\frac{\pi R n}{a}\right)^{2i}, \quad i = 1, 2$  (11)

The remaining coefficient  $w_0$  appearing in (10), which represents the average radial displacement of the artery, is obtained by a simple integration of Eq. (8):

$$w_0 = \frac{R^4 k^2 Q_0}{2D_s a} - \nu \varepsilon_0 R \quad (12)$$

The values  $Q_n$  in the earlier equations represent the Fourier coefficients in the expansion of an external pressure

$$Q_n = \int_{-a}^a p(q) \cos(n\pi q/a) dq \quad (13)$$

Since our intention is to investigate the problem of pressure applied to an artery by a stent, it is worthwhile to consider the specific case of distributed line loading

$$p(q) = Q \delta(q) \quad (14)$$

where  $\delta(q)$  denotes the Dirac-delta function. For this case

$$Q_n = Q \quad n = 0, 1, 2, \dots \quad (15)$$

The magnitude of the average elongation per unit length in the  $x$  direction  $\varepsilon_0$  in Eq. (12) together with the rotation per unit length  $\psi_0$  are derived from the boundary conditions. In the considered problem these conditions are expressed by the conditions of equilibrium in a cross section of the shell perpendicular to the  $x$  axis. In accordance with the assumption that there is no tangential interaction between the stent and the artery, we consider the case of pure normal loading applied to the internal surface of the shell in the radial direction. Therefore, the resultant axial force  $F_x$  and the torque moment  $M_T$  applied to the cross section, which is a circular ring with the radius  $R$ , are equal to zero

$$F_x = 0, \quad M_T = 0 \quad (16)$$

The resultants are expressed in terms of the internal forces calculated per unit length of the ring. Deriving these forces from the obtained expressions for the displacements and carrying out the integration one obtains

$$F_x = 2\pi k(R\varepsilon_0 + \nu w_0) \quad (17)$$

$$M_T = \pi k R^2 (\nu - 1) \psi_0$$

Hence, from the assumptions (16), it follows that the average longitudinal and rotational components of the shell deformations are given by

$$\varepsilon_0 = -\nu \frac{w_0}{R} \quad \text{and} \quad \psi_0 = 0 \quad (18)$$

Consequently, in accordance with (12), the value of  $w_0$  is found to be

$$w_0 = \frac{R^4 k^2 Q_0}{2D_s a(1-\nu^2)} = \frac{Q_0 R^2}{2aEh} \quad (19)$$

Finally, the radial displacement of the artery  $w_a$  along the helix  $q=0$  in accordance with (10) is

$$w_a = \sum_{n=0}^{\infty} w_n \quad (20)$$

where the coefficients  $w_n$  are defined from (11) and (19) and depend upon the applied loading. This loading will be found later from the compatibility conditions for the deformations of a stent and an artery.

Let us now verify the obtained solution by examining a limiting case. Consider the case of the line loading (14) and (15) and assume that the angle  $\alpha$  increases. Then the pitch of the helix  $H$  defining the distance between the loading lines, as it is seen from (1), will decrease and in the limiting situation, when  $\alpha$  approaches 90 deg, the shell will be subjected to the uniform radial pressure  $p_0$  which is the average of the external forces

$$p_0 = \frac{Q}{2a} \quad (21)$$

Substituting the latter relation to (19) (recall, that for the line loading  $Q_0 \equiv Q$ ) one obtains the radial displacement of the shell coinciding with the average value

$$w_0 = \frac{p_0 R^2}{Eh} \quad (22)$$

The last formula represents the well-known solution for the problem of an elastic ring subjected to the internal pressure. The calculations based on the suggested algorithm were carried out for  $\alpha$  close to 90 deg, and the difference from the limiting analytic value (22) was found to be less than 0.1%.

The ratio of the wall thickness to diameter in normal arteries is 0.1. Consequently, the radial compliance determined by means of the thin-walled shell model represents a rather rough approximation. In order to improve the model we will compare the compliances for the thin-walled shell and for the thick hollow cylinder in an auxiliary problem. The obtained difference will be expressed by a coefficient which will correct the solution for the thin-walled shell under helical loading.

In the auxiliary problem the loading to the shell/cylinder inner surface acts not along the helical line but along the periodic system of circular rings perpendicular to the longitudinal axis. The distance between the rings is equal to the pitch  $H$  of the helix. This problem, in contrast to the original one, possesses the axial symmetry and very convenient for a solution.

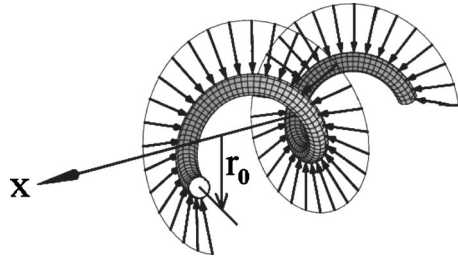


Fig. 3 Curvilinear helical wire subjected to radial loading  $q_n$

The calculations were based on the finite element method. The radial displacement of the thick-walled artery was then obtained from that for a thin-walled shell model (20) using the corrective multiplier equal to the ratio of the corresponding displacements in the auxiliary problem.

### 3 The Stent Model

The second constituent of the considered mechanical system is the Cardiocoil stent [17]. It is depicted in Fig. 3. In order to describe its mechanical behavior we will employ the model of a helical rod (as an inclusion in an elastic matrix) developed by Slepian et al. [24]. The spatial location of the wire is defined by the parameters of the corresponding helix  $r_0, \alpha_0$  passing through the center of the wire cross sections. The curvature  $k_0$  and torsion  $t_0$  of the helix as defined by the use of the Frenet orthogonal coordinates  $\tau, n, b$  shown in Fig. 4 are

$$k_0 = \frac{\sin^2 \alpha_0}{r_0} \quad (23)$$

$$t_0 = \frac{\sin \alpha_0 \cos \alpha_0}{r_0} \quad (24)$$

We will further denote the parameters related to the undeformed (initial) position of the wire by the superscript  $i$ , namely  $r_0^i, \alpha_0^i, k_0^i, t_0^i$ . The principal vector and the principal moment acting at the wire cross section can be presented by the use of their  $s$ -independent components (the  $s$  coordinate is the same as in the previous section)

$$\mathbf{Q} = T\boldsymbol{\tau} + N\mathbf{n} + B\mathbf{b} \quad (25)$$

$$\mathbf{M} = M_\tau\boldsymbol{\tau} + M_n\mathbf{n} + M_b\mathbf{b} \quad (26)$$

One of the initial assumptions of the considered model of the stent-artery interaction is that the tangential stresses at the interface are negligibly small. Consequently, the only external loading applied to the stent is the distributed normal force  $q_n$  directed along the vector  $\mathbf{n}$ . Then from the equilibrium equations it follows that  $N=0, M_n=0$  and

$$k_0 T - t_0 B = -q_n \quad (27)$$

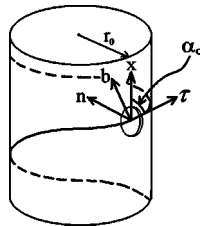


Fig. 4 Frenet orthogonal coordinates used for the stent description

$$k_0 M_\tau - t_0 M_b - B = 0 \quad (28)$$

In addition, since the stent is supposed to be unstressed in the  $x$  direction and untwisted around the  $x$  axis, it may be concluded that  $Q_x=0$  and  $M_x=0$  or

$$T \cos \alpha_0 + B \sin \alpha_0 = 0 \quad (29)$$

$$M_b \sin \alpha_0 + M_\tau \cos \alpha_0 + (T \sin \alpha_0 - B \cos \alpha_0) r_0 = 0 \quad (30)$$

Finally, the elasticity equations relating the stent deformations with the internal moments are given by

$$M_b = EI(k_0 - k_0^i) \quad (31)$$

$$M_\tau = GI_p(t_0 - t_0^i) \quad (32)$$

where  $E, G$  are the Young and the shear modulus of the stent material, respectively,  $I$  is the moment of inertia of the wire cross section about the  $\mathbf{b}$  direction, and  $I_p$  is the polar moment of inertia of the section.

The nonlinear system of Eqs. (23)–(32) completely defined the stress-strain state of the stent and can be employed for deriving its compliance in the radial direction, a property which is of prime importance for the study of stent-artery interaction. This compliance expressed by the dependence  $r_0(q_n)$  is determined in the following way. First, the couples  $r_0, \alpha_0$  providing the solution for Eqs. (23)–(26) and (28)–(32) are found by an incremental procedure with the  $r_0^i, \alpha_0^i$  starting point corresponding to the undeformed position. The obtained values are then substituted in (27) and the magnitude of  $q_n$  corresponding to the given  $r_0$  is calculated. An illustrative numerical result is presented in Fig. 5, in which the dependence of the normalized stent diameter  $d_0$  upon the external line pressure  $q_n$  is depicted. Here, a stent with an outer diameter  $d_0^i=5$  mm and with a helix angle  $\alpha_0^i=81.2$  deg made of a circular wire with a diameter 0.25 mm is considered. The material of the stent is NiTiNol with an elastic modulus  $E=46.6$  GPa and a Poisson ratio  $\nu=0.3$ . The type of the nonlinearity with a positive second derivative in the working region  $3 \text{ mm} < d_0 < 5 \text{ mm}$  conforms with the experimental results presented by Jedwab and Clerc [14] for a stent composed of several helices. The information on the decreasing of the external pressure for a very large stent deformations is understood from the physical considerations and probably may be used in studying stent delivery problem. The longitudinal stent deformation in the  $x$  direction is defined by the deviation of the helix angle  $\alpha_0$  from its initial value  $\alpha_0^i$ . The dependence of  $\alpha_0$  upon the external pressure is found to be similar to the behavior of  $d_0$ .

Additional support for the validity of the developed stent model comes from experimental results of Schrader and Beyar [9]. The compliance of stents was experimentally investigated in that study and expressed in terms of the external pressure  $p_r$  and the radial deformation  $\varepsilon_r$ . A comparison of the analytical and the experimental results for the NiTiNol stent with an external diameter 3 mm, a helix angle  $\alpha_0^i=81.2$  deg and a wire cross section  $0.09 \times 0.12$  mm is presented in Fig. 6. The agreement is reasonably good, the difference that does exist may be explained by the effect of the shear stresses at the loaded surface of the stent which are present in the experimental device and are absent in the analytical model. Consequently, the pressure required in the experiment to reach the specific stent radial contraction is higher.

### 4 Stent-Artery Interaction

In developing a suitable model for stent interaction with a diseased artery we have to take into account the role of plaque in diminishing the width of arterial lumen. In the clinical setting, balloon angioplasty is usually carried out before the stent insertion in order to bring the inner diameter  $\bar{d}_{\text{dis}}^{\text{in}}$  of the diseased artery to the size  $d_{\text{dis}}^{\text{in}}$  which is equal to the inner diameter of a healthy artery  $d_{\text{heal}}^{\text{in}}$ . As a result, the preinflation situation in which the

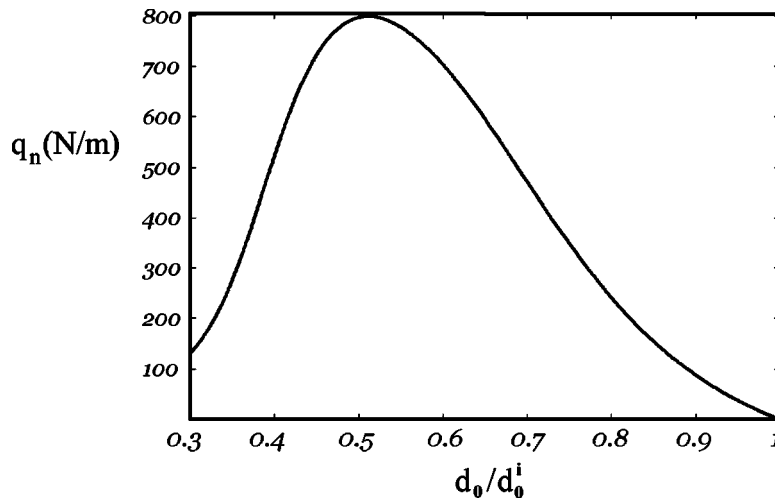


Fig. 5 The influence of the external radial line pressure  $q_n$  on the normalized outer stent diameter  $d_0$

outer diameters of the diseased and the healthy arteries are equal but the inner diameters are different reverts to the situation in which the inner diameters are the same but the outer ones are different. The outer diameter  $d_{dis}^{out}$  of the diseased artery is then determined from mass conservation

$$(\bar{d}_{dis}^{out})^2 - (\bar{d}_{dis}^{in})^2 = (d_{dis}^{out})^2 - (d_{dis}^{in})^2 \quad (33)$$

The tube obtained after inflation will include the arterial tissue and the existing plaque. The elastic properties of the sick artery are significantly influenced by the disease. According to Holzapfel [15] the increase in the isotropic elastic response of the some parts of the Intima may approach 150%, a certain change takes place even in Media and only Adventitia remains unaltered. Nevertheless we will assume here that the tube material may be considered as isotropic elastic with the same elastic properties as those of a healthy artery. The earlier simplifying assumptions are somewhat presumptuous, but we contend that they are reasonable within the framework of the present study to obtain the first-approximation analytical results.

Stent-artery interaction lends itself well to study by means of a model. The self-expanding stent and the postinflation artery can be considered as two elastic springs. Inserting one into another

leads to a stress-strain state that appears as the result of a geometric mismatch between the springs (i.e., the outer diameter of the stent exceeds the inner diameter of the artery) and the external force (i.e., the blood pressure). Note that one of the springs (the stent) is assumed nonlinear. The nonlinear elastic response of the NiTiNol coil stent is caused by the geometrical nonlinearity, and we take this into account. In contrast, for the artery model the physical nonlinearity may have an importance; we, however, use the linearly elastic model. The determination (and the account) of the artery physical nonlinearity seems to be an important task in this field.

The compatibility condition that needs to be fulfilled at the stent-artery interface has the form

$$d_{dis}^{in} + 2w_a = d_0^i + 2w_s \quad (34)$$

where  $w^a$  and  $w^s$  are the respective radial displacements of the artery and the stent at the interface, and  $d_0^i$  is the outer diameter of the stent in the unloaded position. The displacements which are caused by the average blood pressure  $p_b$  and by the pressure  $p_{sa}$  at the stent-artery interface, can be easily calculated using the results for the radial compliances obtained in the previous sections.

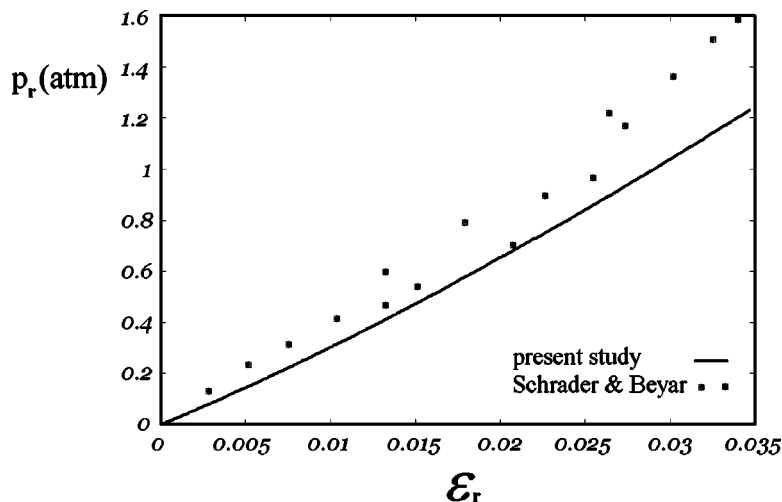


Fig. 6 The external radial pressure on the stent  $p_r$  vs relative radial contraction  $\epsilon_r$  for the 3 mm stent with the rectangular cross section  $0.09 \times 0.12$  mm

**Table 1 Interaction of arteries having 75% area stenosis with 3 mm (a) and 5 mm (b) stents.**

(a)				
Inner diameter of inflated artery before stenting (mm)		2.90	2.70	2.50
Difference between the stent and the artery diameters- $\Delta d$ (mm)		0.10	0.30	0.50
Circular cross section	Artery diameter after stent implantation (mm)	2.93	2.83	2.71
	Damage factor- $D$	4.23	13.0	23.11
Rectangular cross section	Artery diameter after stent implantation (mm)	2.92	2.75	2.60
	Damage factor- $D$	1.95	6.78	12.94
(b)				
Inner diameter of inflated artery before stenting (mm)		4.90	4.70	4.50
Difference between the stent and the artery diameters- $\Delta d$ (mm)		0.10	0.30	0.50
Circular cross section	Artery diameter after stent implantation (mm)	4.93	4.82	4.71
	Damage factor- $D$	2.82	7.8	13.26
Rectangular cross section	Artery diameter after stent implantation (mm)	4.91	4.73	4.56
	Damage factor- $D$	1.02	2.93	5.35

The unknown interface pressure  $p_{sa}$  is derived by a simple trial-and-error procedure in order to fulfill (34). A damage factor characterizing the level of forces acting between the stent and arterial surfaces is defined as the normalized interface pressure

$$D = \frac{P_{sa}}{P_b} \quad (35)$$

A parametric study of this factor will be presented in the following section.

### 5 Numerical Results

The manufacturer's recommendation for choosing the stent diameter for a specific patient is based mainly on the mismatch between the outer radius of the stent and the inner radius of the artery. On the other hand, the same radial mismatch may lead to very different contact pressures (and, consequently, damage factors that defines arterial injury), depending upon the compliance of the stent, the diameter of the artery and the percent of stenosis. This is important for choosing the correct therapeutic solution. The numerical results presented later illustrate the earlier dependencies for the Cardiocoil stent.

The damage factors for stents with rectangular and circular cross sections are given in Table 1. Two standard outer stent diameters of 3 mm (Table 1a) and 5 mm (Table 1b) are considered. Accordingly, circular wires have diameters of 0.15 and 0.25 mm, and the dimensions of the rectangular cross section are  $0.09 \times 0.12$  mm and  $0.135 \times 0.18$  mm. The results are calculated for three radial stent-artery mismatches  $\Delta d = 0.1, 0.3, 0.5$  mm which correspond to the healthy arteries with diameters 2.9, 2.7, 2.5 mm, respectively, for Table 1a, and 4.9, 4.7, 4.5 mm for Table 1b. The area stenosis is assumed to be 75% for all the cases. The results show that the increase of the lumen after stent implantation grows monotonically with the increase of the radial mismatch and approaches the maximum value of 0.21 mm for the circular wire and 0.1 mm for the rectangular one (Table 1a). The smaller extent of increase in the latter case is understandable since the rectangular wire stent is more compliant. Consequently, the damage factor for this stent is found to be significantly less than that for the stent with a circular cross section. Specifically, for the maximal radial mismatch 0.5 mm the difference between the damage factors is about 240% for the 5 mm stents and 180% for the 3 mm ones.

Moreover, it can be noted that the damage factor seems to be proportional to the radial stent-artery mismatch. This fact is illus-

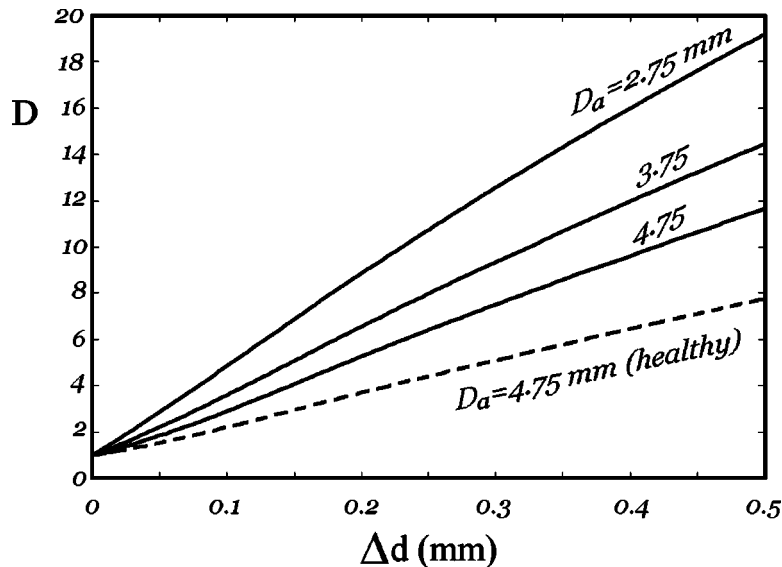


**Fig. 7 Dependence of the damage factor  $D$  upon the radial stent-artery mismatch  $\Delta d$  for the case of a circular wire. The arterial diameter is fixed and the stent diameter is varied for each curve. The dashed line corresponds to the healthy 4.75 mm artery.**

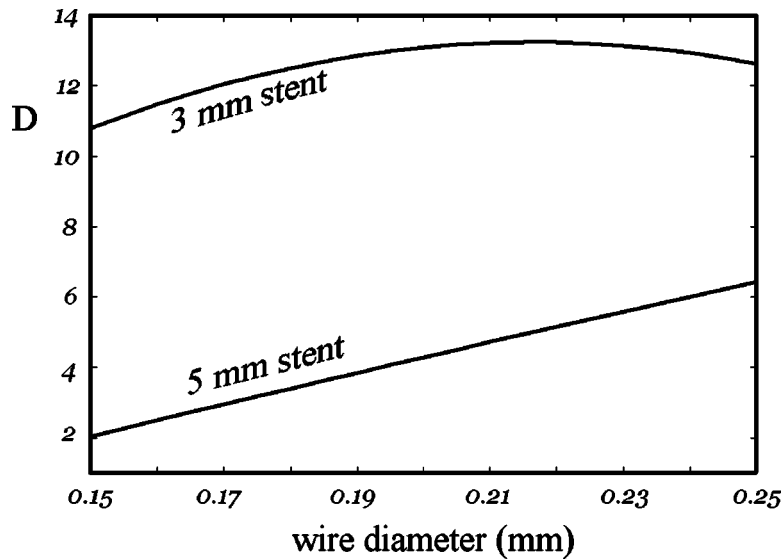


Fig. 8 Dependence of the damage factor upon the wire's diameter for the 3 mm diameter and 5 mm diameter stents, the radial mismatch with the artery is 0.25 mm

trated by the data presented in Fig. 7 which presents  $D$  for injured arteries of 2.75, 3.75, and 4.75 mm with 75% stenosis. The graph for the healthy artery is also given for reference. The dependence of the damage factor upon the mismatch is found to be very close to linear. For the limiting value  $\Delta d=0$  when the outer diameter of the stent is equal to the inner diameter of the artery, the contact pressure under the stent is, in fact, equal to average blood pressure. Consequently, the stent-artery interaction vanishes and, in accordance with (35), the damage factor in this case is equal to unity.

The influence of the stent geometry on the damage factor for 75% area stenosis is presented in Figs. 8 and 9. In the former, the diameter of the circular wire varies. The results for the 3 and 5 mm stents with a 0.25 mm radial mismatch reveal a general trend of moderate increasing of the damage factor with increasing of the wire diameter. This phenomenon is in agreement with the fact that

enlarging of the wire diameter leads to the increasing of the radial stiffness of the stent. On the other hand, when the wire becomes thicker, the stent-artery contact area increases as well, which may decrease the contact stresses that define the damage factor. The latter observation helps to understand the reduction of the damage factor for the 3 mm stent observed for large wire diameters. The two mentioned effects of stent radial stiffening and increasing of the interface contact area having the opposite influence on the contact stresses explain the nonmonotonic behavior of the damage factor as a function of the helix angle  $\alpha$  (Fig. 9). It is interesting to note that for the circular wire stent, the maximum is seen for the angles in the vicinity of 80 deg, and this is the value for the Cardiocoil stents currently employed in clinical practice.

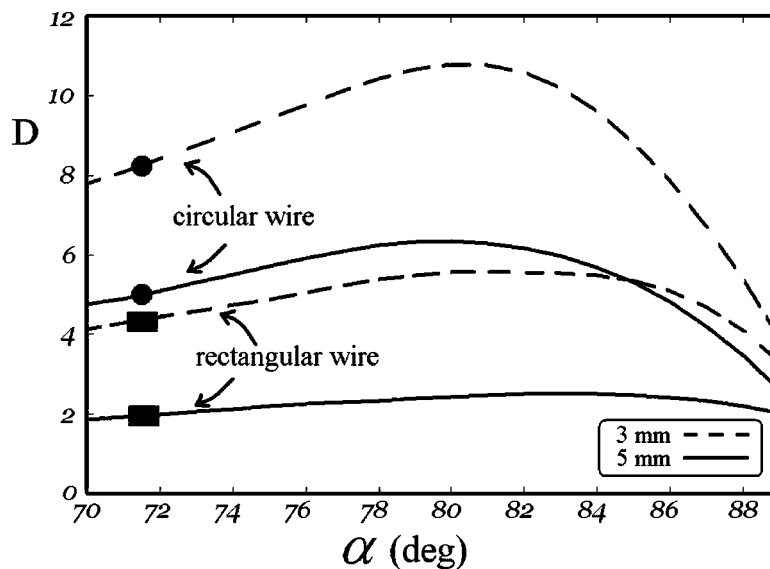


Fig. 9 Dependence of the damage factor upon the helix angle  $\alpha$  (in the undeformed position) for the 3 mm (dashed lines) and 5 mm (solid lines) stents. The radial mismatch with the artery is 0.25 mm for all the cases.

## 6 Concluding Remarks

The study of the stent-artery interaction phenomenon is a complicated mechanical problem. It requires developing a three-dimensional model for a system including the constituents of different origin (steel, tissue, plaque) characterizing by a nonlinear behavior and having a large gap in geometric and elastic properties. In addition, the data defining these properties are usually known with a limited accuracy. Consequently, a pure numerical approach to the problem requires tremendous computational effort and the results in the literature are usually presented only for specific parameter combinations.

The approach suggested in the present study is different. In order to understand the basic mechanics of the interaction problem several rather presumptuous simplifying assumptions have been made. In particular, the material of the injured artery is considered as linear isotropic elastic one, the prestretching of the artery in the circumferential and longitudinal directions is ignored, the influence of stent ends on the stress state is neglected. This enabled to develop a very efficient semi-analytical model of interaction of the artery with Cardiac coil stent and carry out a parametric study. The interaction is characterized by a *damage factor* defined as the ratio of the contact stresses at the stent-artery interface to average blood pressure. It is obvious that this factor cannot be either too small or too large: if it is too small, the interaction between the stent and the artery is absent and the stent does not fulfill its supporting function, and if it is too large, the arterial injury may lead to growth of neointima and restenosis. In spite of the simplifying assumptions the obtained results are believed to give an acceptably accurate description of the differences in the damage factor resulting from the variation in the properties of the stent and of the artery. Establishing of an optimal value for this factor based on an analysis of known data collected from medical experience is an important topic for future studies.

The results we obtained for the Cardiac coil stent can be applied by the designers of this type of stent as well as by medical personnel for choosing the most suitable stent for a specific patient. Future research should include analytical/numerical derivation of damage factors for other stent types and investigation of the influence of plaque geometry on the damage factor.

## Acknowledgment

This work was partly supported by Nicholas and Elisabeth Slezak Super Center.

## References

- [1] Werner, G. S., Bahrmann, P., Mutschke, O., Emig, U., Betge, S., Ferrari, M., and Figulla, H. R., 2003, "Determinants of Target Vessel Failure in Chronic Total Coronary Occlusions after Stent Implantation—The Influence of Collateral Function and Coronary Hemodynamics," *J. Am. Coll. Cardiol.*, **42**(2), pp. 219–225.
- [2] De Belder, A., and Thomas, M. R., 1998, "The Pathophysiology and Treatment of In-stent Restenosis," *Stent*, **1**(3), pp. 74–82.

- [3] Akiyama, T., Di Mario, C., Reimers, B., Ferraro, M., Moussa, I., Blengino, S., and Colombo, A., 1997, "Does the High-Pressure Stent Expansion Induce More Restenosis?," *J. Am. Coll. Cardiol.*, **29**, p. 368A.
- [4] Oesterle, S. N., Whitbourn, R., Fitzgerald, P. J., Yeung, A. C., Stertzer, S. H., Dake, M. D., Yock, P. G., and Virmani, R., 1997, "The Stent Decade: 1987 to 1997," *Am. Heart J.*, **136**, pp. 578–599.
- [5] Rachev, A., 1997, "Theoretical Study of the Effect of Stress-Dependent Remodeling on Arterial Geometry under Hypertensive Conditions," *J. Biomech.*, **30**, pp. 819–827.
- [6] Rachev, A., Manoach, E., Berry, J., and Moore, J. E., Jr., 2000, "A Model of Stress-Induced Geometrical Remodeling of Vessel Segments Adjacent to Stents and Artery/Graft Anastomoses," *J. Theor. Biol.*, **206**, pp. 429–443.
- [7] Fluecker, F., Sternthal, H., and Klein, G. E., 1994, "Strength, Elasticity, and Plasticity of Expandable Metal Stents: In Vitro Studies with Three Types of Stents," *J. Vasc. Interv. Radiol.*, **5**, pp. 745–750.
- [8] Lossef, S. V., Luts, R. J., and Mandorf, J., 1994, "Comparison of Mechanical Deformation Properties of Metallic Stents with Use of Stress-Strain Analysis," *J. Vasc. Interv. Radiol.*, **5**, pp. 341–349.
- [9] Schrader, C. S., and Beyar, R., 1998, "Evaluation of the Compressive Mechanical Properties of Endoluminal Metal Stents," *Cathet. Cardiovasc. Diagn.*, **44**, pp. 179–187.
- [10] Dyet, J. F., Watts, G., Ettles, D. F., and Nicholson, A. A., 2000, "Mechanical Properties of Metallic Stents: How Do These Properties Influence the Choice of Stent for Specific Lesions?," *Cardiovasc. Intervent. Radiol.*, **23**, pp. 47–54.
- [11] Etave, F., Finet, G., Boivin, M., Boyer, J., Rioufol, G., and Thollet, G., 2001, "Mechanical Properties of Coronary Stents Determined by Using Finite Element Analysis," *J. Biomech.*, **34**, pp. 1065–1075.
- [12] Dumoulin, C., and Cochelin, B., 2000, "Mechanical Behavior Modeling of Balloon-Expandable Stents," *J. Biomech.*, **33**, pp. 1461–1470.
- [13] Loshakove, A., and Azhari, H., 1997, "Mathematical Formulation for Computing the Performance of Self Expanding Helical Stents," *Int. J. Med. Inf.*, **44**, pp. 127–133.
- [14] Jedwab, M. R., and Clerc, C. O., 1993, "A Study of the Geometrical and Mechanical Properties of a Self-Expanding Metallic Stent—Theory and Experiment," *J. Appl. Biomater.*, **4**, pp. 77–85.
- [15] Holzapfel, G. A., Stadler, M., and Schulze-Bauer, C. A. J., 2002, "A Layer-Specific Three-Dimensional Model for the Simulation of Balloon Angioplasty using Magnetic Resonance Imaging and Mechanical Testing," *Ann. Biomed. Eng.*, **30**, pp. 753–767.
- [16] Auricchio, F., Di Loreto, M., and Sacco, E., 2001, "Finite Element Analysis of a Stenotic Artery Revascularization through a Stent Insertion," *Comput. Methods Biomechanics and Biomechanical Engineering*, **4**, pp. 249–264.
- [17] *Handbook of Coronary Stents*, P. Serruys, ed., Martin Dunitz, London, 1996, Chap. 10.1.
- [18] Beyar, R., Henry, M., Shofti, R., Grenadier, E., Globerman, E., and Beyar, M., 1994, "Self Expandable Nitinol Stent for Cardiovascular Applications: Canine and Human Experience," *Cathet. Cardiovasc. Diagn.*, **32**, pp. 162–170.
- [19] Grenadier, E., Shofti, S., Beyar, M., Lichtig, H., Mordechovitz, D., Globerman, O., Markiewicz, W., and Beyar, R., 1994, "Self Expandable and Highly Flexible Nitinol Stent: Immediate and Long Term Results in Dogs," *Am. Heart J.*, **128**, pp. 870–878.
- [20] Hong, M. K., Beyar, R., Kornowski, R., Tio, F. O., Bramwell, O., and Leon, M. B., 1997, "Acute and Chronic Effects of Self-Expanding Nitinol Stents in Porcine Coronary Arteries," *Coron. Artery Dis.*, **8**(1), pp. 45–48.
- [21] Roguin, A., Grenadier, E., Linn, S., Markiewicz, W., and Beyar, R., 1999, "Continued Expansion of the Nitinol Self-Expanding Coronary Stent: Angiographic Analysis and One-Year Clinical Follow-Up," *Am. Heart J.*, **138**(2), pp. 326–333.
- [22] Holzapfel, G. A., Eberlein, R., Wriggers, P., and Wezsäcker, H. W., 1996, "Large Strain Analysis of Soft Biological Membranes: Formulation and Finite-Element Analysis," *Comput. Methods Appl. Mech. Eng.*, **132**, pp. 45–61.
- [23] Vinson, J. R., 1993, *The Behavior of Shells Composed of Isotropic and Composite Materials*, Kluwer Academic, the Netherlands.
- [24] Slepian, L. I., Krylov, V. I., and Parnes, R., 2000, "Helical Inclusion in an Elastic Matrix," *J. Mech. Phys. Solids*, **48**, pp. 827–865.